Electronic Supplementary Material (ESI) for Dalton Transactions.
This journal is © The Royal Society of Chemistry 2024

Supporting Information

Dual Nodes Bridged Cobalt-modified Keggin-type Polyoxometalate-based Chain for Highly Efficient CO_2 Photoconversion

Xin-Lian Chen, Jie-Wu, Ji-Lei Wang, Xiao-Mei Liu, Hua Mei*, and Yan Xu*[,a]

[a] College of Chemical Engineering, State Key Laboratory of Materials-Oriented Chemical Engineering, Nanjing Tech University, Nanjing 211816, P. R. China
Coordination Chemistry Institute, State Key Laboratory of Coordination Chemistry, Nanjing University, Nanjing 210093, PR. China.

Contents

Materials and methods

All chemical reagents were commercially available and utilized directly without further purification. On a Bruker D8X diffractometer, measurements of powder X-ray diffraction (PXRD) were made using Cu-K_α (λ = 1.5418 Å) at room temperature with a scan speed of 10° min^{-1}. Using a Perkin-Elmer 2400CHN elemental analyzer, the elements of C, H, and N were determined. Additionally, FT-IR spectra were collected by KBr pellets and a Nicolet Impact 410 FTIR spectrometer in the range of 4000-400 cm^{-1}. On a scanning X-ray microprobe (PHI 5000 *Verasa*, ULAC-PHI, Inc.) using an Al-K (1486.6 eV) achromatic X-ray source, X-ray photoelectron spectroscopy studies were performed.

Synthesis

It has been established that the hydro-/solvothermal approach performs well for constructing novel POM-based hybrid complexes recently. The development of POM-base compounds is influenced by various parameters during the synthesis process, including temperature, solvent diversity, reaction duration, and pH. In addition, we should pay attention to the fact that compounds exhibit high reproducibility during preparation. As a result, it is practical to differentiate them based on their color and shape, as illustrated in Figure S1. Table 1 presents the complete crystallographic information for these three compounds.

X-ray crystallography

The crystal XRD data of three compounds was collected at 296(3) K on Bruker Apex II CCD with Mo-K_α radiation (λ = 0.71073 Å). The SHELX software package was utilized to resolve and refine the structure of compounds through the direct method and full-matrix least-squares method on F^2 in the SHELX-2018/3 program package. In addition, the non-H atoms were refined by anisotropic thermal parameters. The detailed crystallographic data of two compounds are summarized in Table 1. Main bond lengths and bond angles of three compounds were provided in Tables S1-S3. Crystallographic data have been deposited with the Cambridge Crystallographic Data Centre (CCDC) as 2359927 (**$SiW_{12}Co_2$**), 2359929 (**$SiW_{12}Ni_2$)** and 2359928 (**$SiW_{12}Mn_2$**).

Mott-Schottky plot measurements.

All electrochemical measurements (Mott–Schottky plot, Photocurrent) were carried out *via* a conventional three-electrode system in a 0.2 M Na_2SO_4 aqueous solution (pH = 6.8). The conductive glass, carbon rod and saturated Ag/AgCl electrode were considered as the working electrode, counter electrode, and reference electrode, respectively. The preparation of the working electrode was given as follows: catalyst of 2 mg was ground to powder and then dispersed in anhydrous ethanol (990 μL) in the presence of 10 μL 5% Nafion solution by ultrasonication to form a homogeneous ink. Subsequently, 200 μL of the ink was deposited onto the carbon cloth (S = 1 cm × 2 cm), and dried at room temperature for Mott-Schottky spots measurements. The Mott–Schottky plots were measured over an alternating current

(AC) frequency of 1500 Hz, 2000 Hz and 2500 Hz, and three electrodes were immersed in the 0.2 M Na_2SO_4 aqueous solution.

Photocurrent responsive measurements.

The photoelectrochemical characterizations were performed on the electrochemical workstation (CHI 760e) with the assembled photoelectrodes as the working electrode, the Pt mesh as the counter electrode and the Ag/AgCl as the reference electrode. Meanwhile, the 0.2 M Na_2SO_4 aqueous solution was filled in the cell as the electrolyte. The light source and density were identical with that in the CO_2 photoreduction experiments.

Photocatalytic CO_2 reduction measurement

CO_2 photoreduction tests were performed on an evaluation system (CEL-SPH2N-S9, AULTT, China), in a 100 mL quartz container, and irradiated with a 300 W Xe lamp, which intensity of light is 5.2×10^5 cd ($420 \leq \lambda \leq 800$ nm). A specific amount of catalysts were dispersed in 40 mL of MeCN aqueous solution, $[Ru(bpy)_3]Cl_2\cdot6H_2O$ (0.015 mmol) as a photosensitizer, TEOA (10 mL) as a sacrificial reagent, and transferred them into a glass container. Then, the container was saturated with high-purity CO_2 gas, repeated three times, and the reaction system temperature was ensured at 6 ℃ *via* a circulating water-cooling system outside the container. After reaction finished, the amounts of gaseous products (CO, CH_4 and H_2) were analyzed using a gas chromatography equipped with a flame ionization detector (FID), and a thermal conductivity detector (TCD).

Recycling experiments.

Reusability and stability are important indicators to evaluate catalyst, after each reaction, the catalyst was recovered by centrifugation and washed several times with deionized water and then dried at 80 ℃ for 12 h before the next reaction.

Supplementary Structural Information

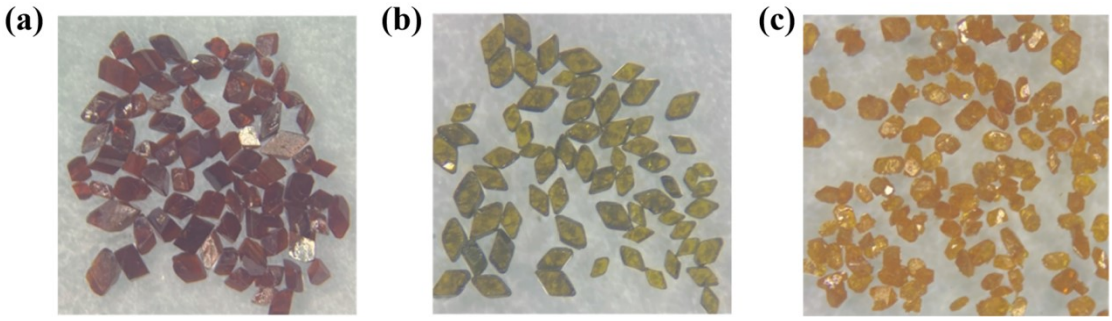

Figure S1. The images of three compounds under an optical microscope.

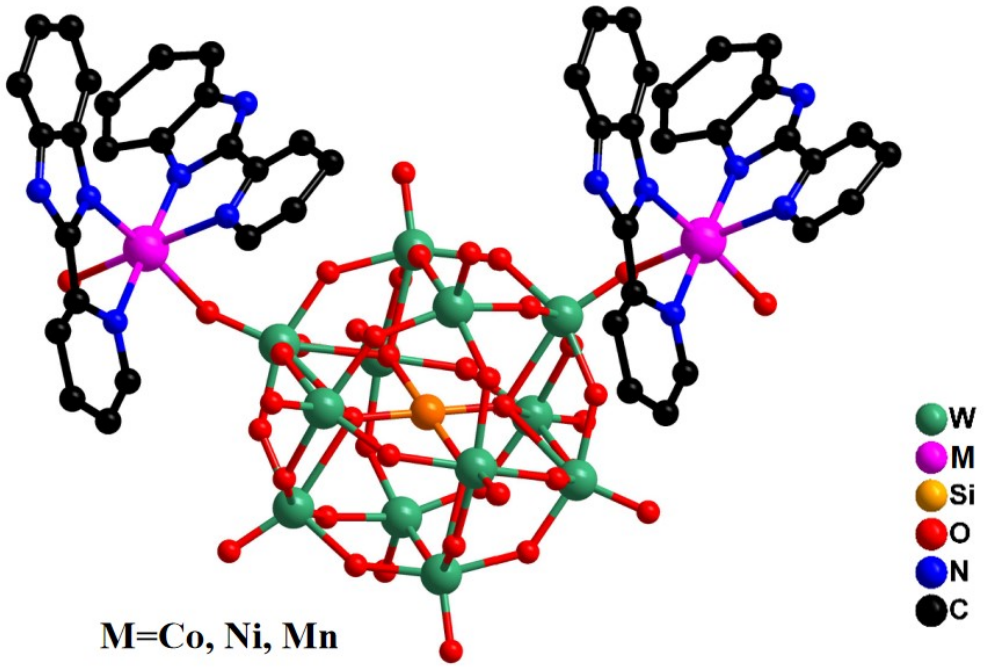

Figure S2. The asymmetric unit of **$SiW_{12}M_2$**.

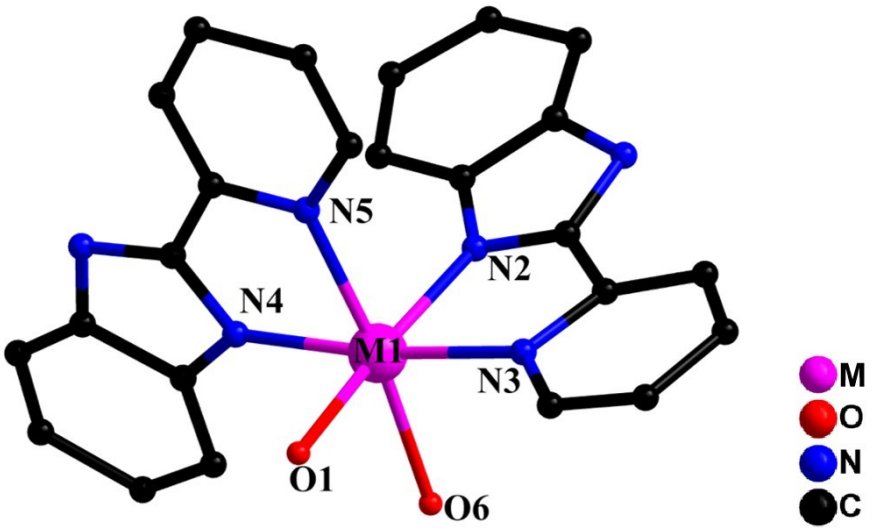

Figure S3. Local coordination environments of {M} atom in **$SiW_{12}M_2$**.

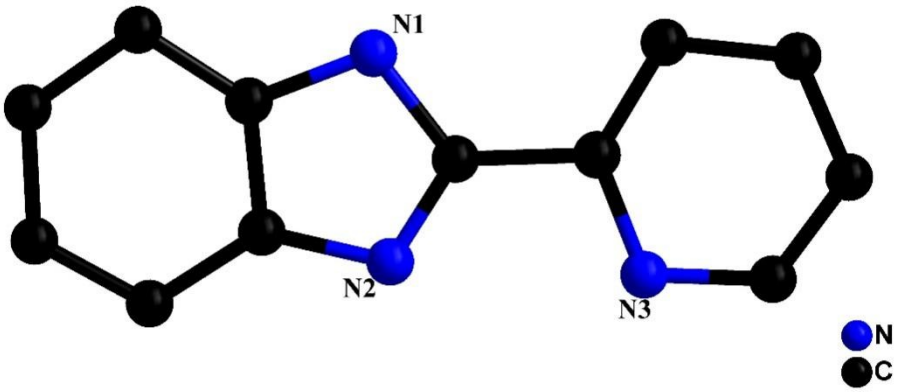

Figure S4. Basic units of ligands.

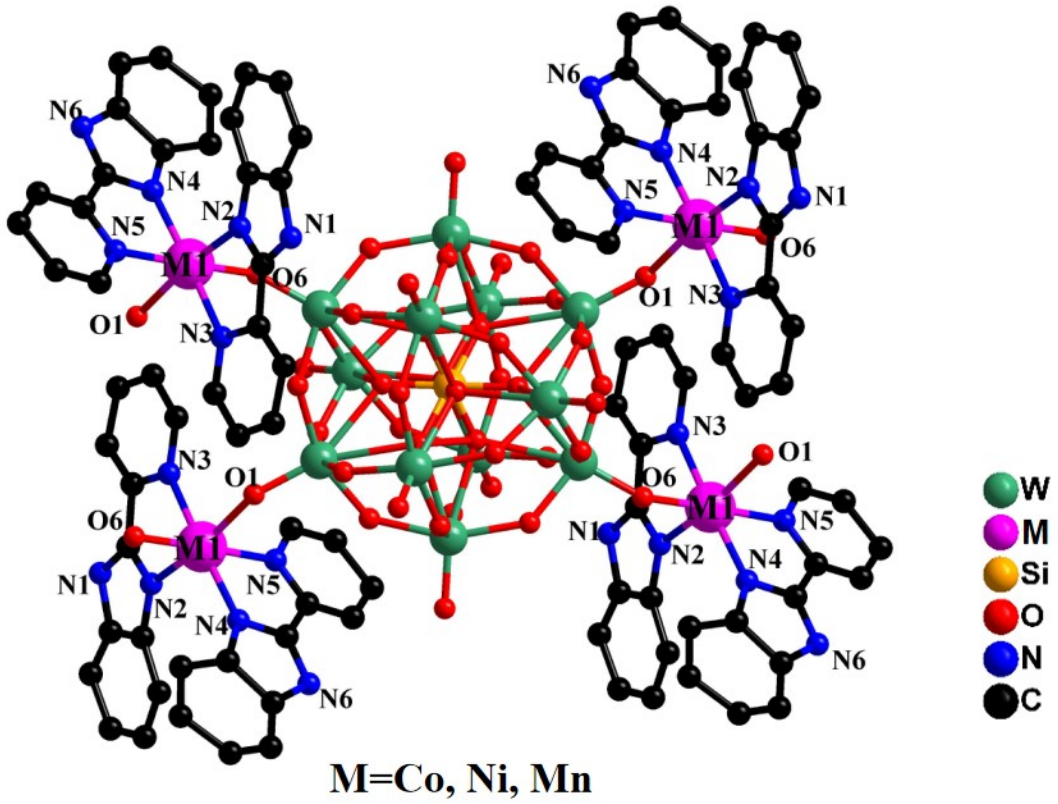

Figure S5. Local coordination environments of **$SiW_{12}M_2$** unit.

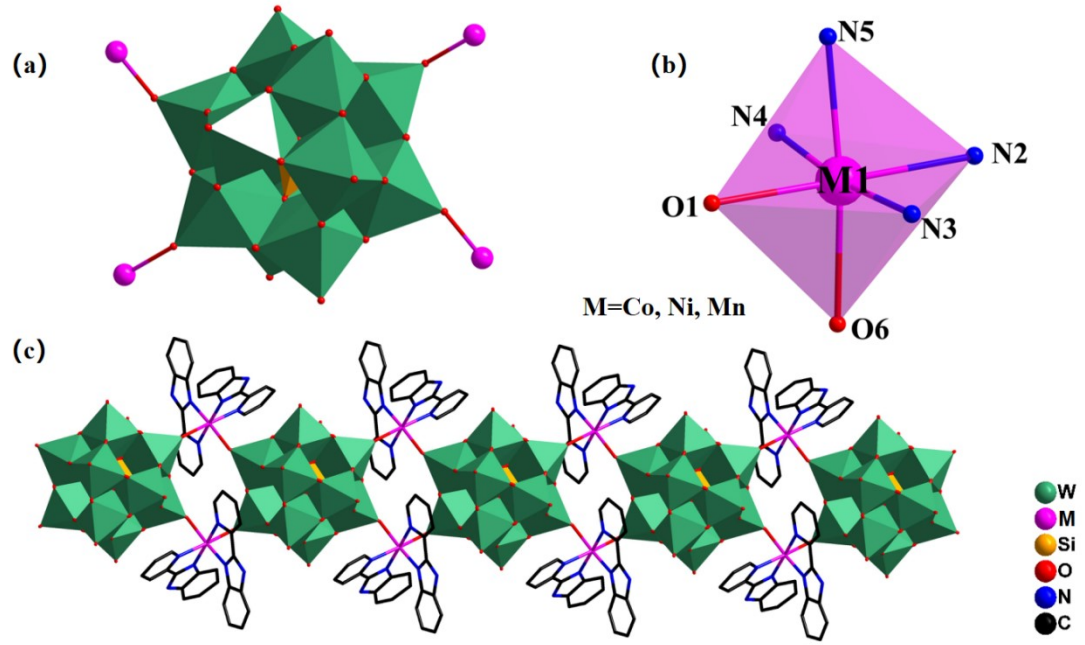

Figure S6. The structure of **$SiW_{12}M_2$** (Co, Ni, Mn): (a) 4-connected {$SiW_{12}O_{40}$}; (b) the coordination environment of Co; (c) the 1D chain.

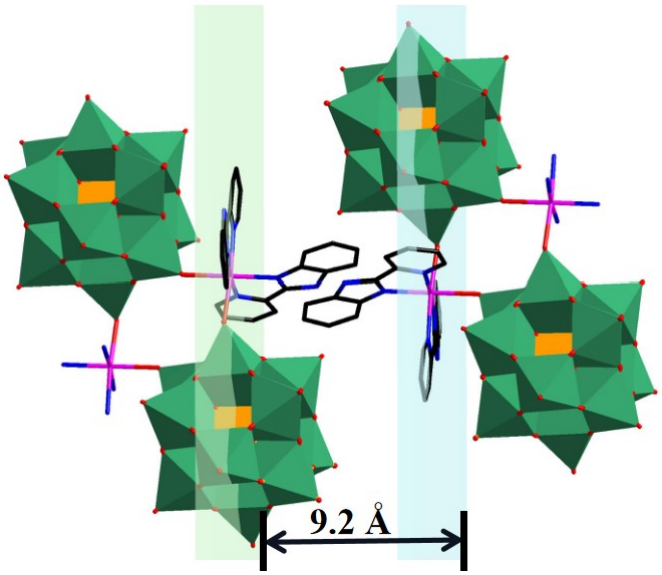

Figure S7. The distance form 2D layers through π-π stacking interactions between pyim ligands.

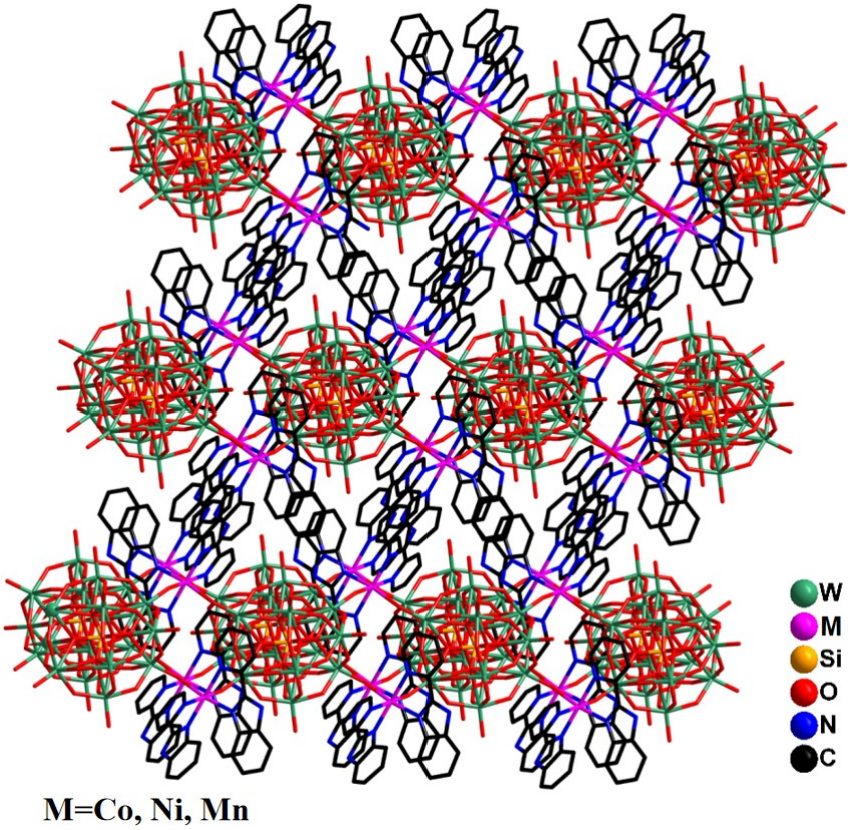

Figure S8. The 3D supramolecular framework of **$SiW_{12}M_2$**.

Supplementary Characterization Information

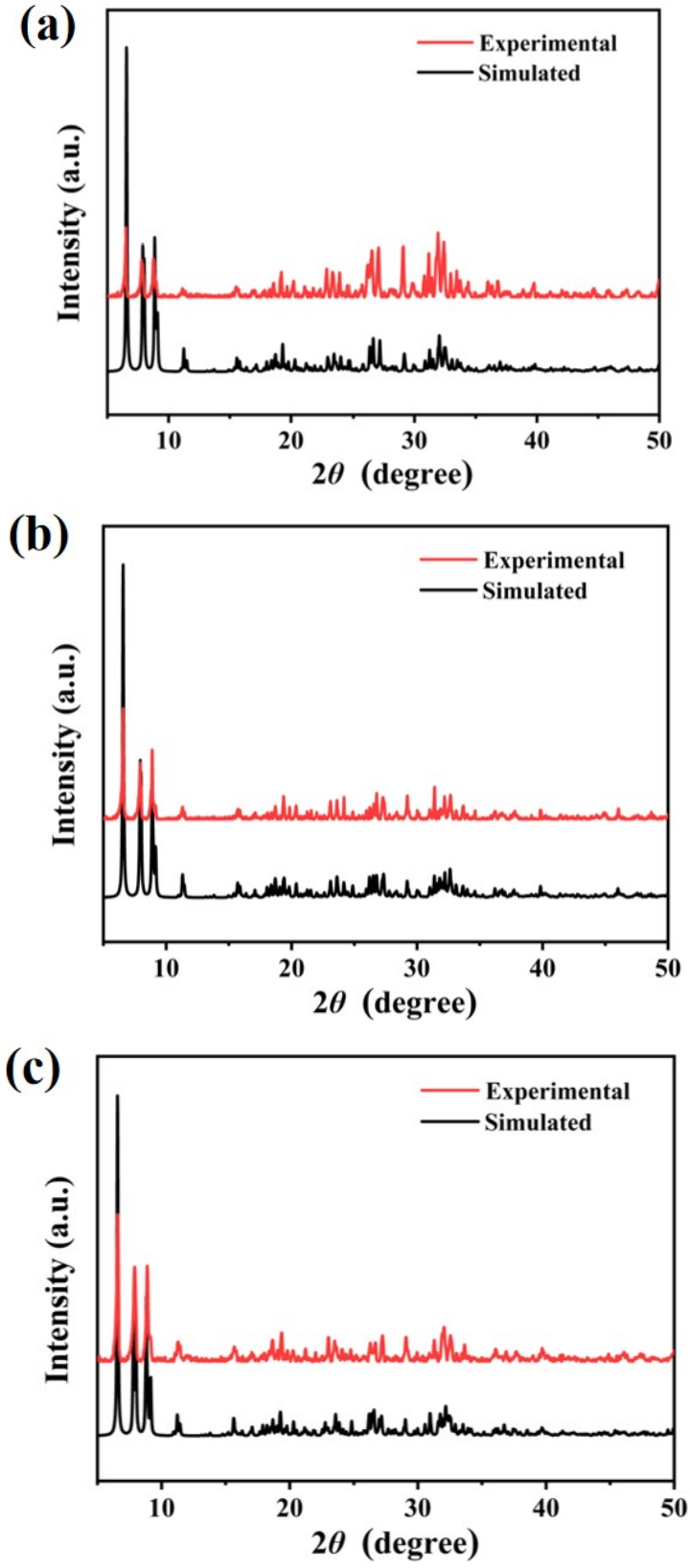

Figure S9. Experimental and theoretical XRD patterns of three compounds (a-c).

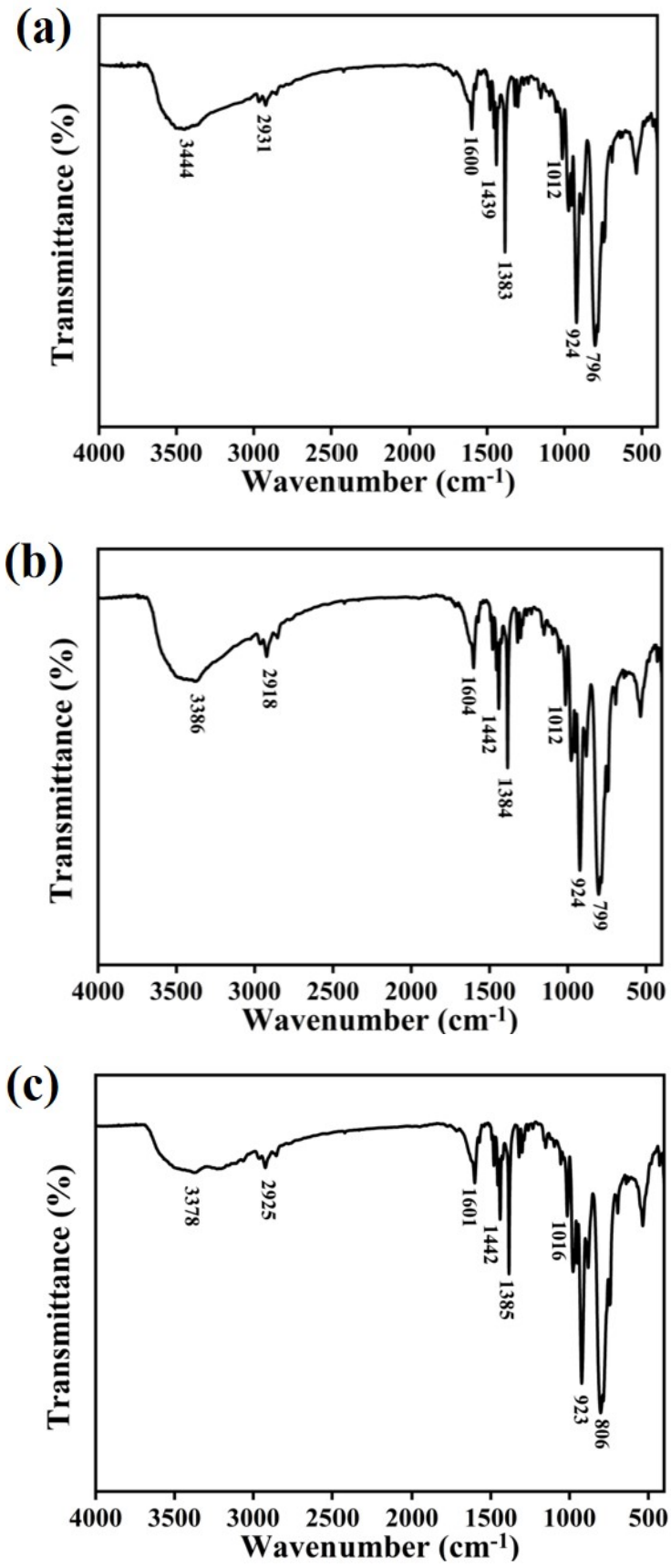

Figure S10. The IR spectra of three compounds (a-c).

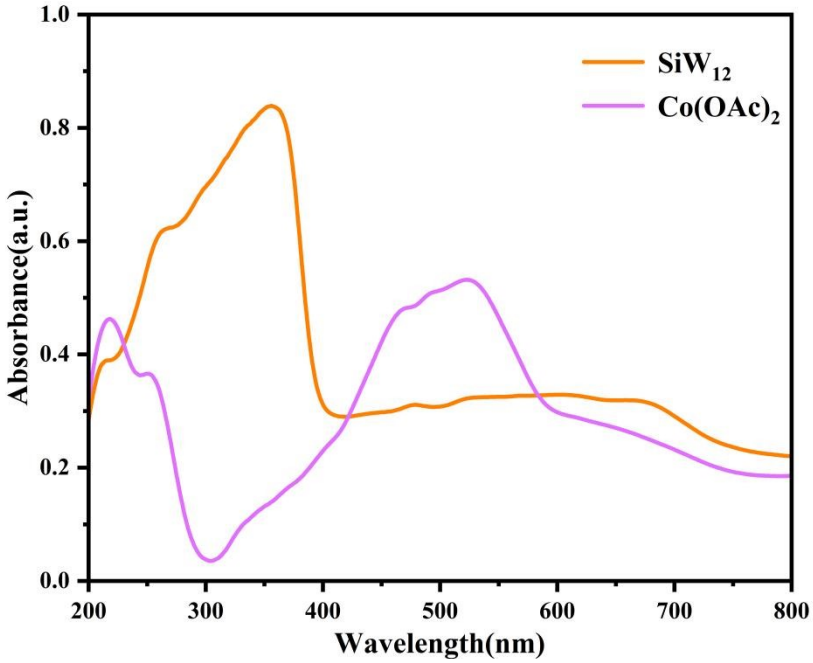

Figure S11. The UV-Vis spectra of SiW_{12} and $Co(OAc)_2$.

.

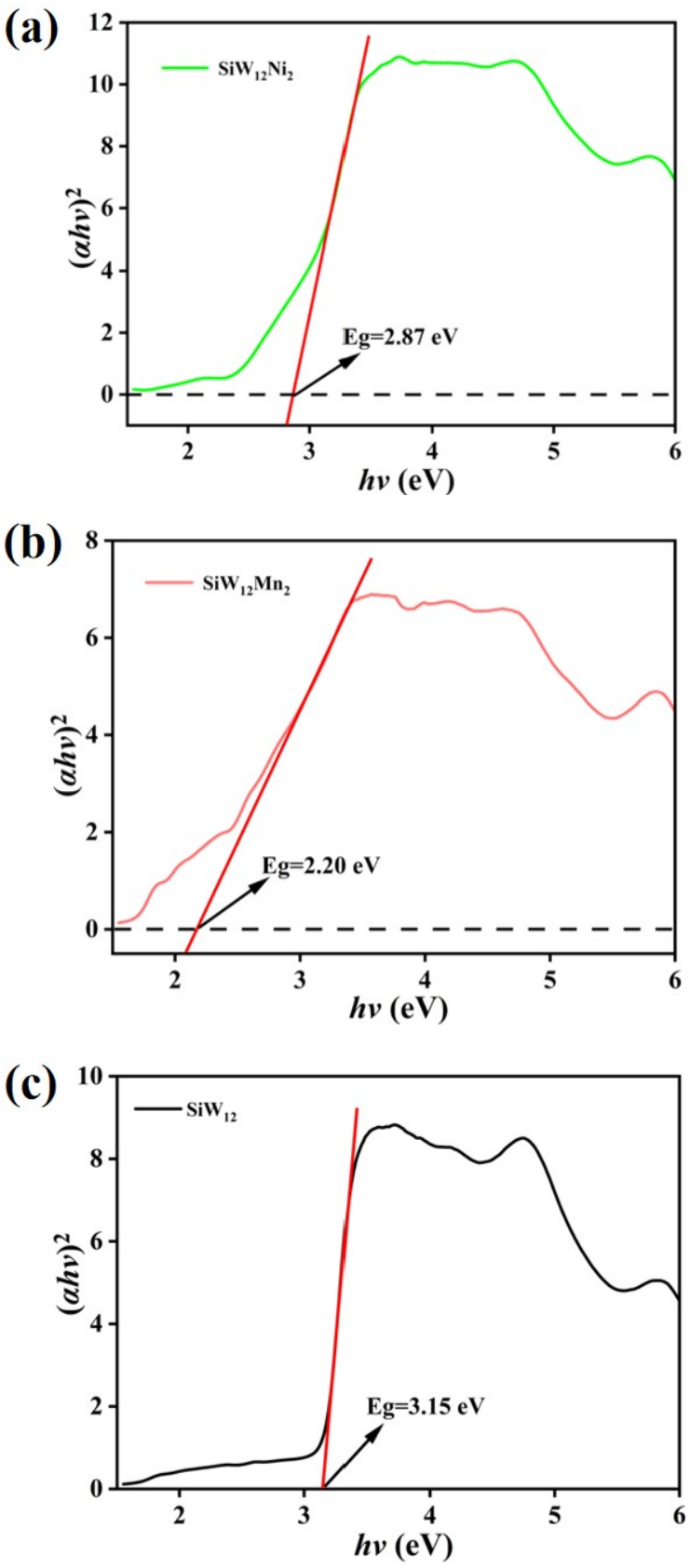

Figure S12. The Tauc plot of $(\alpha h\nu)^2$ *vs*. hν for **$SiW_{12}Ni_2$**, **$SiW_{12}Mn_2$** (a-b) and SiW_{12} (c).

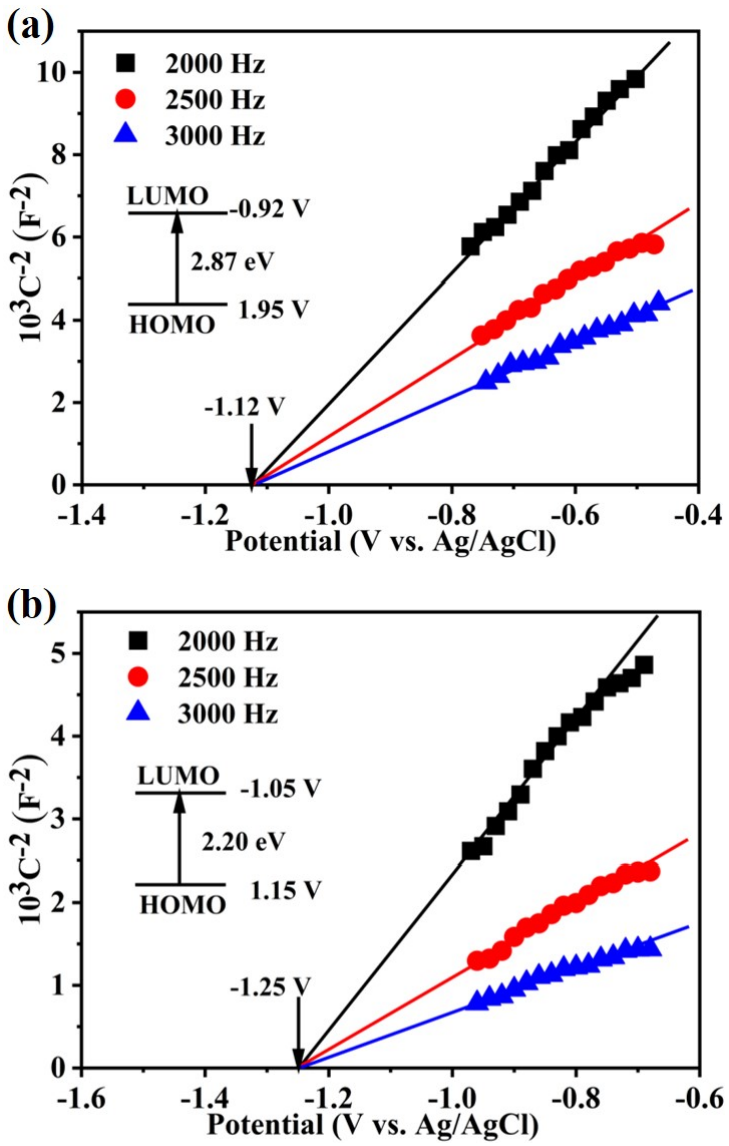

Figure S13. Mott-Schottky plot for **$SiW_{12}Ni_2$** and **$SiW_{12}Mn_2$** (a-b).

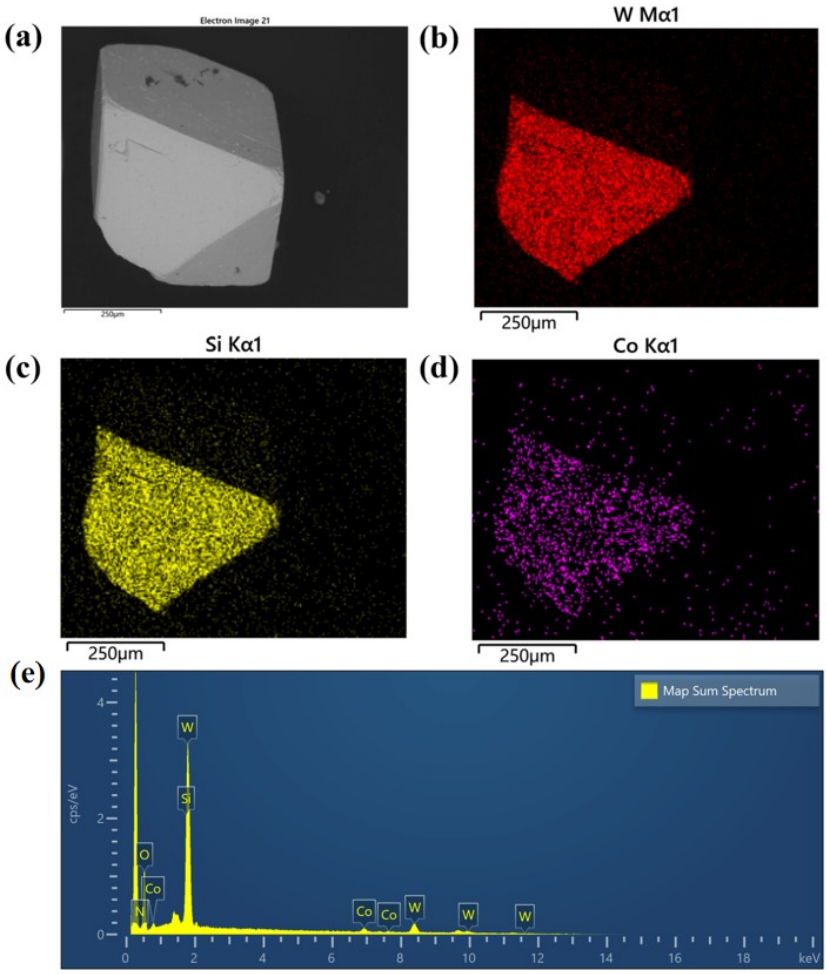

Figure S14. The SEM image (a), the corresponding SEM-EDS elemental mapping of W, Si, Co elements (b-d) and the map sum spectrum (e) of **$SiW_{12}Co_2$**.

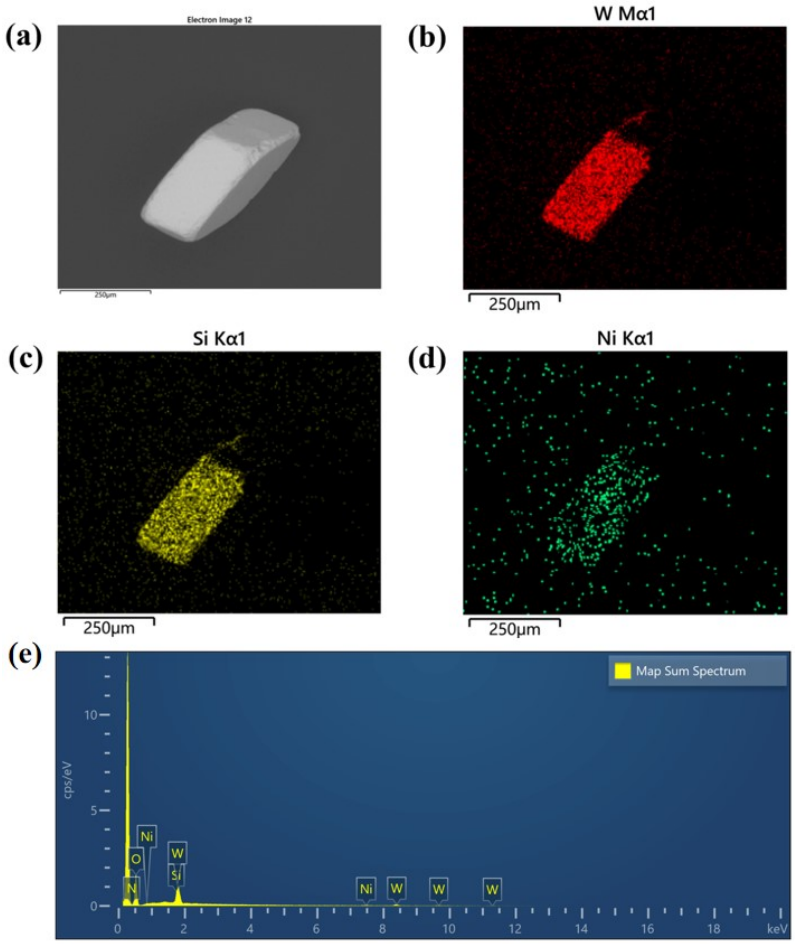

Figure S15. The SEM image (a), the corresponding SEM-EDS elemental mapping of W, Si, Ni elements (b-d) and the map sum spectrum (e) of **$SiW_{12}Ni_2$**.

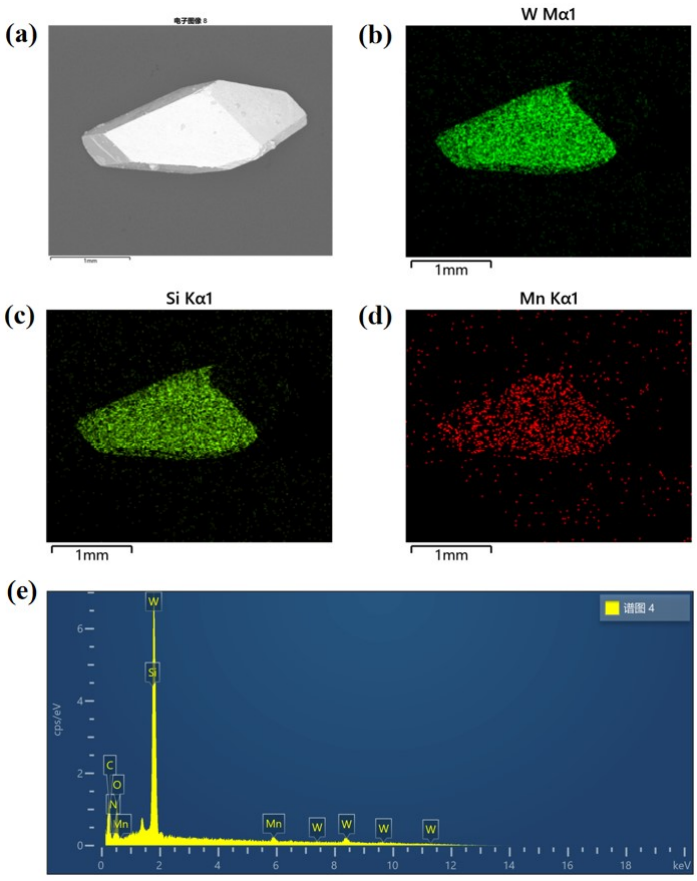

Figure S16. The SEM image (a), the corresponding SEM-EDS elemental mapping of W, Si, Mn elements (b-d) and the map sum spectrum (e) of **$SiW_{12}Mn_2$**.

Supplementary CO_2 Photoreduction

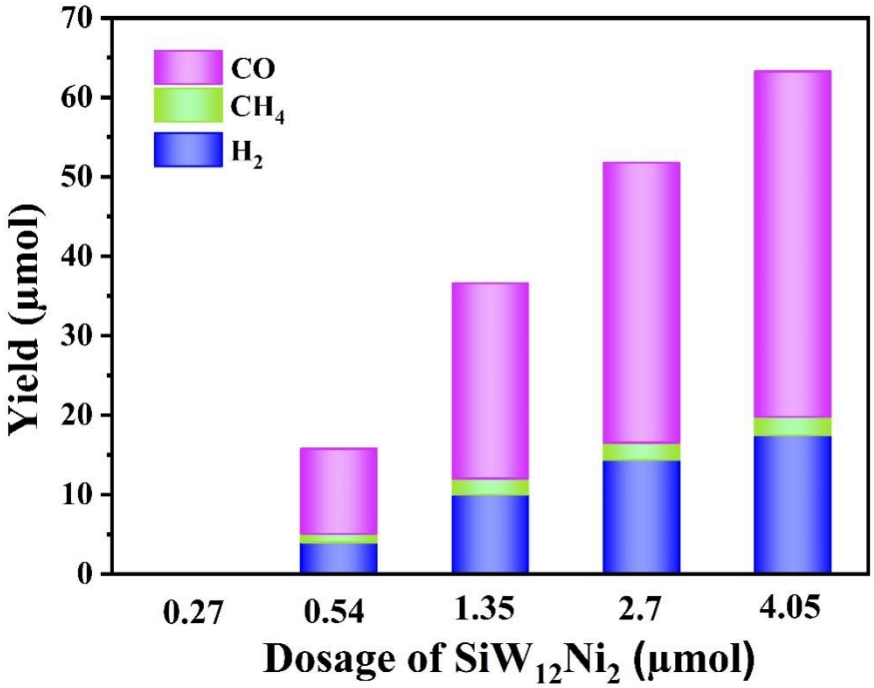

Figure S17. The effect of different amounts of **$SiW_{12}Ni_2$** on the production of CO and H_2.

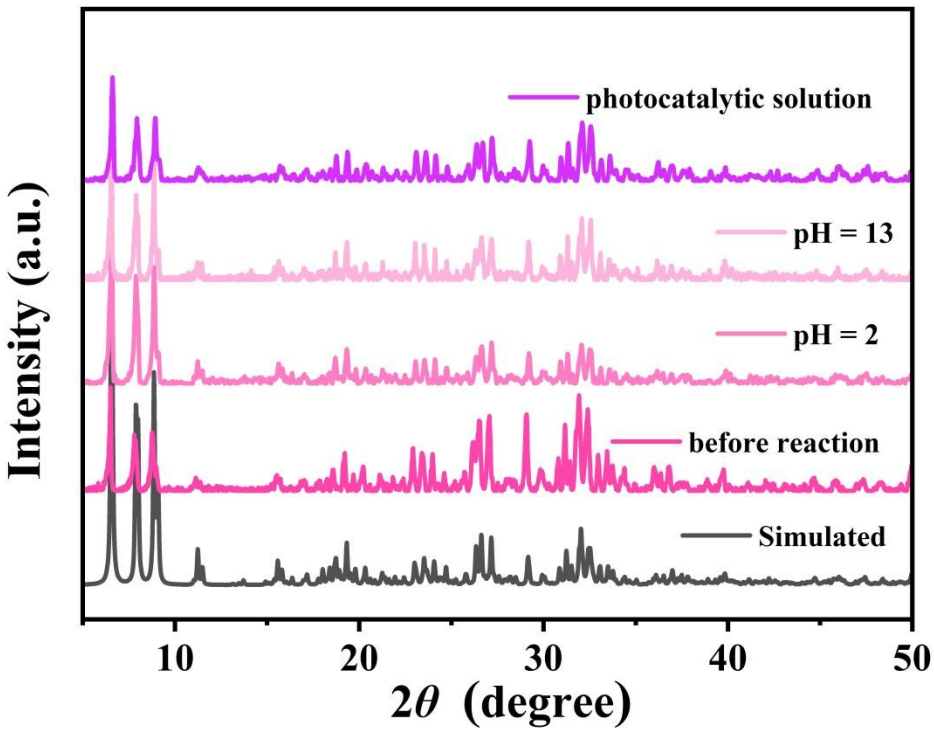

Figure S18. PXRD patterns of $SiW_{12}Co_2$ under the conditions of the specified pH values and photocatalytic reaction solution by soaking the samples for 24 h.

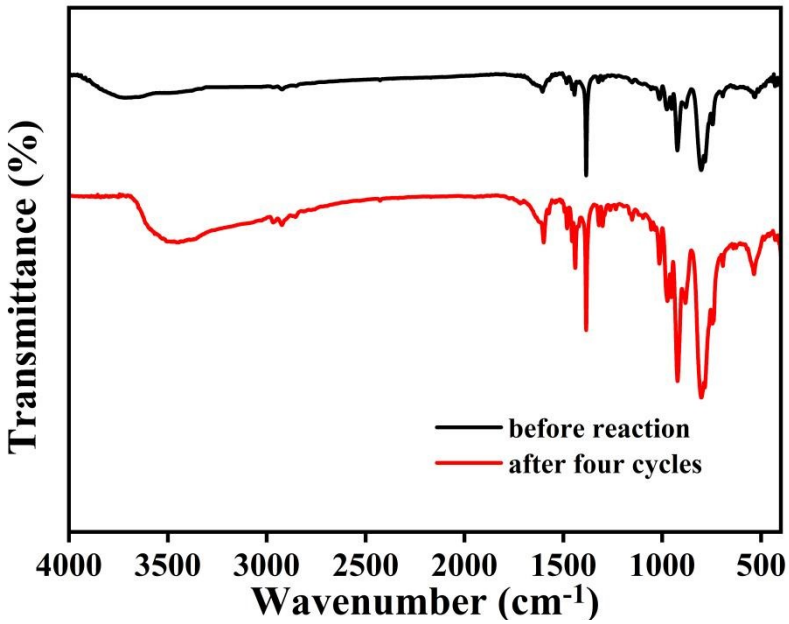

Figure S19. The IR spectra of $SiW_{12}Co_2$ before reaction and after four cycles.

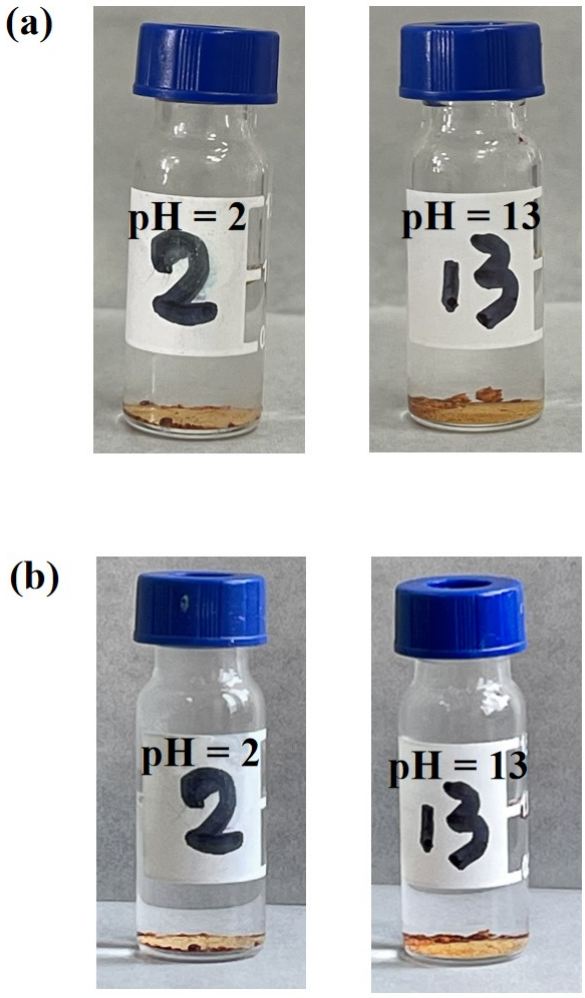

Figure S20. The images of $SiW_{12}Co_2$ soaked in solutions with different pH before and after 24 hours.

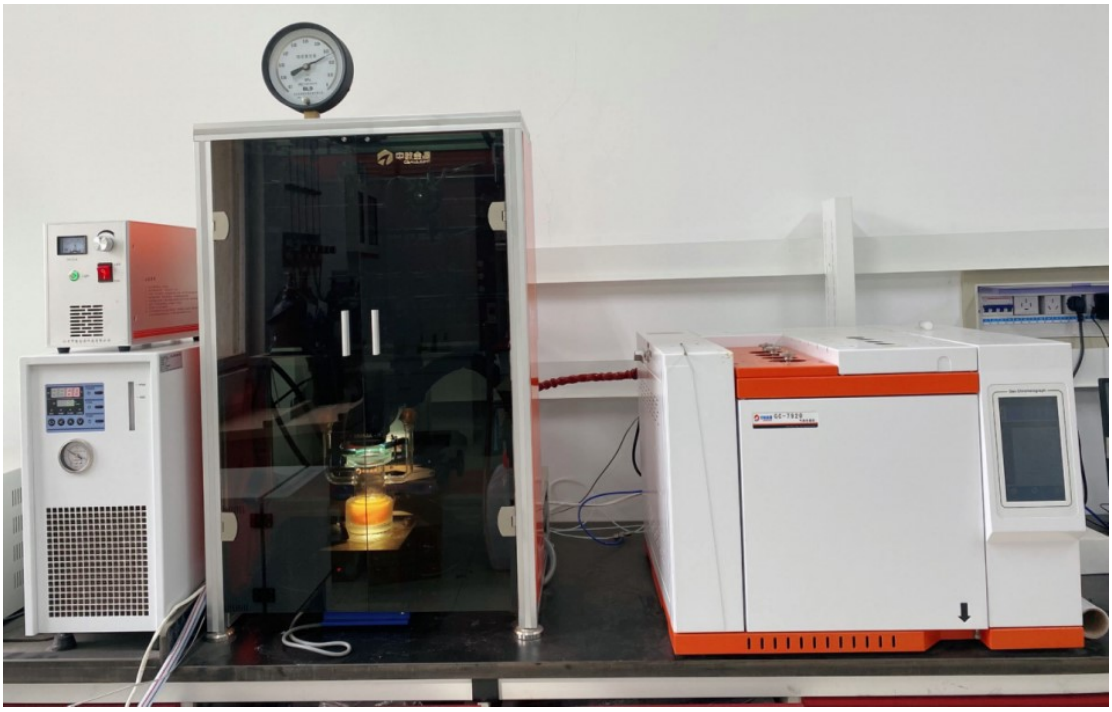

Figure S21. The reaction device for CO_2 photoreduction.

Supplementary Tables

Table S1: Selected bond lengths (Å) and bond angles (˚) for **$SiW_{12}Co_2$**。

W(1)-O(8)	1.90(2)	Si(1)-O(22)#1	1.65(3)
W(1)-O(9)	1.677(17)	O(1)-Co(1)-O(6)#2	86.5(6)
W(1)-O(10)	1.91(2)	O(1)-Co(1)-N(5)	89.8(5)
W(1)-O(11)	1.859(18)	N(2)-Co(1)-O(1)	169.3(5)
W(1)-O(17)	1.886(17)	N(2)-Co(1)-O(6)#2	97.6(6)
W(1)-O(12)	2.40(3)	N(2)-Co(1)-N(3)	78.2(2)
W(1)-O(21)	2.41(4)	N(2)-Co(1)-N(5)	86.8(5)
Co(1)-O(1)	2.168(15)	N(3)-Co(1)-O(1)	92.1(5)
Co(1)-O(6)#2	2.193(15)	N(3)-Co(1)-O(6)#2	88.6(5)
Co(1)-N(2)	2.107(7)	N(3)-Co(1)-N(5)	96.2(4)
Co(1)-N(3)	2.143(8)	N(4)-Co(1)-O(1)	90.8(5)
Co(1)-N(4)	2.065(7)	N(4)-Co(1)-O(6)#2	97.2(5)
Co(1)-N(5)	2.178(8)	N(4)-Co(1)-N(2)	98.5(3)
Si(1)-O(12)#1	1.63(3)	N(4)-Co(1)-N(3)	173.7(4)
Si(1)-O(20)	1.64(3)	N(4)-Co(1)-N(5)	78.2(2)
Si(1)-O(21)	1.58(4)	N(5)-Co(1)-O(6)#2	174.1(5)

Symmetry transformations used to generate equivalent atoms: #1 (-x, -y+1, -z); #2 (x+1, y, z)

Table S2: Selected bond lengths (Å) and bond angles (˚) for **$SiW_{12}Ni_2$**.

W(1)-O(9)	1.688(17)	Si(1)-O(12)	1.63(3)
W(1)-O(17)	1.87(2)	O(1)-Ni(1)-O(6)#2	86.5(6)
W(1)-O(11)	1.87(2)	N(4)-Ni(1)-O(1)	90.8(5)
W(1)-O(10)	1.92(2)	N(4)-Ni(1)-O(6)#2	95.6(4)
W(1)-O(8)	1.93(2)	N(5)-Ni(1)-O(1)	89.8(5)
W(1)-O(12)	2.36(4)	N(5)-Ni(1)-O(6)#2	174.7(5)
W(1)-O(21)	2.38(3)	N(2)-Ni(1)-O(1)	172.7(5)
Ni(1)-O(1)	2.157(15)	N(2)-Ni(1)-O(6)#2	95.4(6)
Ni(1)-O(6)#2	2.205(16)	N(3)-Ni(1)-O(1)	92.2(5)
Ni(1)-N(4)	2.017(6)	N(3)-Ni(1)-O(6)#2	88.2(5)
Ni(1)-N(2)	2.065(7)	N(2)-Ni(1)-N(3)	80.9(2)
Ni(1)-N(3)	2.097(7)	N(2)-Ni(1)-N(5)	88.7(4)
Ni(1)-N(5)	2.122(8)	N(3)-Ni(1)-N(5)	95.8(4)
Si(1)-O(20)	1.60(3)	N(4)-Ni(1)-N(2)	96.0(3)
Si(1)-O(21)	1.61(3)	N(4)-Ni(1)-N(3)	175.3(3)
Si(1)-O(22)	1.60(3)	N(4)-Ni(1)-N(5)	80.6(2)

Symmetry transformations used to generate equivalent atoms: #1 (-x, -y+1, -z); #2 (x+1, y, z)

Table S3: Selected bond lengths (Å) and bond angles (˚) for **$SiW_{12}Mn_2$**.

W(1)-O(9)	1.679(15)	Si(1)-O(22)	1.65(2)
W(1)-O(17)	1.885(17)	N(4)-Mn(1)-N(2)	96.8(2)
W(1)-O(11)	1.905(16)	N(4)-Mn(1)-O(1)	94.4(5)
W(1)-O(10)	1.91(2)	N(2)-Mn(1)-O(1)	165.8(5)
W(1)-O(8)	1.920(19)	N(4)-Mn(1)-O(6)#2	100.2(4)
W(1)-O(12)	2.40(3)	N(2)-Mn(1)-O(6)#2	99.1(6)
W(1)-O(21)	2.43(3)	O(1)-Mn(1)-O(6)#2	87.5(6)
Mn(1)-N(4)	2.173(6)	N(4)-Mn(1)-N(3)	167.6(3)
Mn(1)-N(2)	2.215(7)	N(2)-Mn(1)-N(3)	75.91(19)
Mn(1)-O(1)	2.225(15)	O(1)-Mn(1)-N(3)	91.5(4)
Mn(1)-O(6)#2	2.238(14)	O(6)#2-Mn(1)-N(3)	91.0(5)
Mn(1)-N(3)	2.259(7)	N(4)-Mn(1)-N(5)	74.81(18)
Mn(1)-N(5)	2.307(8)	N(2)-Mn(1)-N(5)	85.4(4)
Si(1)-O(12)	1.60(3)	O(1)-Mn(1)-N(5)	89.0(4)
Si(1)-O(21)	1.58(3)	O(6)#2-Mn(1)-N(5)	173.7(4)

Symmetry transformations used to generate equivalent atoms: #1 (-x, -y+1, -z); #2 (x+1, y, z)

Table S4: Comparison of the performance of the POM-based photocatalysts for CO_2 reduction.

Photocatalyst	Photosensitizer Sacrificial agent	$Rate_{CO}$ (μmol g^{-1} h^{-1})	$Rate_{H2}$ (μmol g^{-1} h^{-1})	System	Ref.
$SiW_{12}Co_2$	$[Ru(bpy)_3]Cl_2·6H_2O$ triethanolamine	10733	6100	heterogeneous	This work
$SiW_{12}Ni_2$	$[Ru(bpy)_3]Cl_2·6H_2O$ triethanolamine	1129	120	heterogeneous	This work
$H_{26.5}K_{2.5}Na$ $(H_2O)_{16}$-$[Ni_6(OH)(BO_3)_2(dien)_2(B\text{-}\alpha\text{-}SiW_{10}O_{37})_2]_2·24H_2O$	$[Ru(bpy)_3]Cl_2·6H_2O$ triethanolamine	6988	1315	—	[1]
$H_7Na_{19}(H_2O)_{26}\{Ni_{12}(OH)_9$-$(PO_4)_4(A\text{-}\alpha\text{-}SiW_9O_{34})$ $[W_4O_{10}(OH)(PO_2(OH)_2)_2$-$(A\text{-}\alpha\text{-}SiW_9O_{34})_2]\}$ $4C_2H_8N·27H_2O·$	$[Ru(bpy)_3]Cl_2·6H_2O$ triethanolamine	1950	410	—	[1]
$[Co(en)_2]_6[V_{12}B_{18}O_{54}$-$(OH)_6]·17H_2O$	$[Ru(bpy)_3]Cl_2·6H_2O$ triethanolamine	5700	3800	heterogeneous	[2]
$[Ni(en)_2]_6[V_{12}B_{18}O_{54}$-$(OH)_6]·17H_2O$	$[Ru(bpy)_3]Cl_2·6H_2O$ triethanolamine	3200	300	heterogeneous	[2]
CoO-$[(n\text{-}C_4H_9)N]_4Mo_8O_{26}$-UNWs	$[Ru(bpy)_3]Cl_2·6H_2O$ triethanolamine	4165	11555	heterogeneous	[3]
$[Co_{2.67}(SiW_{12}O_{40})(H_2O)_4$-$(Htrz)_4]·Cl_{1.33}$	$[Ru(bpy)_3]Cl_2·6H_2O$ triethanolamine	5235	4841	heterogeneous	[4]
$[Co_3(SiW_{12}O_{40})(H_2O)_3(Htrz)_6Cl]·Cl·6H_2O$	$[Ru(bpy)_3]Cl_2·6H_2O$ triethanolamine	6167	6066	heterogeneous	[4]
$Na_{10}Co_4(H_2O)_2(PW_9O_{34})_2$-@g-$C_3N_4$	—	89.6	5.8	heterogeneous	[5]
$Na_6[Co(H_2O)_2(H_2tib)]_2\{Co$-$[Mo_6O_{15}(HPO_4)_4]_2\}·5H_2O$	—	1.07	—	heterogeneous	[6]
$Na_3[Co(H_2O)_3][Co_2(bib]$-$(H_2bib)_{2.5}\{HCo[Mo_6O_{14}(OH)(HPO_4)_4]_2\}·4H_2O$	—	0.94	—	heterogeneous	[6]

Reference

1. Y. Chen, Z. W. Guo, Y. P. Chen, Z. Y. Zhuang, G. Q. Wang and G. Y. Yang, *Inorg. Chem. Front.*, 2021, **8**, 1303-1311.
2. X. Yu, C. C. Zhao, J. X. Gu, C. Y. Sun, H. Y. Zheng, L. K. Yan, M. Sun, X. L. Wang and Z. M. Su, *Inorg. Chem.*, 2021, **60**, 7364-7371.
3. H. Z. Yang, D. R. Yang and X. Wang, *Angew. Chem., Int. Ed. Engl.*, 2020, **59**, 15527-15531.
4. W. Yao, C. Qin, N. Xu, J. Zhou, C. Y. Sun, L. Liu and Z. M. Su, *CrystEngComm*, 2019, **21**, 6423-6431.
5. J. Zhou, W. C. Chen, C. Y. Sun, L. Han, C. Qin, M. M. Chen, X. L. Wang, E. B. Wang and Z. M. Su, *ACS Appl. Mater. Interfaces*, 2017, **9**, 11689-11695.
6. J. Du, Y. Y. Ma, X. Xin, H. Na, Y. N. Zhao, H. Q. Tan, Z. G. Han, Y. G. Li and Z. H. Kang, *Chem. Eng. J.*, 2020, **398**, 125518.